Journal of Metallurgy and Materials Science, Vol. 63, No. 1-2, January-June 2021, pp. 61-73
Printed in India, © NML, ISSN 0972-4257

Effect of aging on hardness and tensile properties of advanced Mg-Sn based alloys

SONIKA[1], A P MURUGESAN[2], DEBDAS ROY[1], PALASH PODDAR[3]
[1] Department of Materials and Metallurgical Engineering, National Institute of Foundry and Forge Technology, Ranchi-834003, India.
[2]Materials Engineering Division, CSIR-National Metallurgical Laboratory, Jamshedpur-831007, India
[3] CSIR-National Metallurgical Laboratory, Jamshedpur-831007, India

ABSTRACT : The aim of the investigation is to study the effect of aging on as-cast Mg-10Sn (wt%) (T10), Mg-10Sn-3Al (wt%) (TA103) and Mg-10Sn-3Al-1Zn (wt%) (TAZ1031) alloys. Ageing was conducted at 200°C for the duration of 100h and 500h. Vickers hardness and tensile test were conducted at room temperature to examine the mechanical properties of the as-cast and aged alloys. In as-cast condition, Mg-10Sn (wt%) consisted of Mg_2Sn intermetallic phases only while the addition of 3% Al resulted in the precipitation of an additional phase, $Mg_{17}Al_{12}$. The addition of 3% Al and 1% Zn in as-cast alloy assisted the formation of secondary phase and refined the grain size which engendered improvement in hardness and tensile property. Besides that, adding Al and Zn also enhanced precipitation hardening response, it promoted the formation of fine precipitates during ageing process and significantly increased the area fraction of secondary phase. Mg-10Sn-3Al (wt%) shows YS, UTS and % elongation values of 120 MPa, 201 MPa and 60.23% respectively. As compared to as cast condition, aged Mg-10Sn-3Al (wt%) and Mg-10Sn-3Al-1Zn (wt%) exhibited higher hardness value by ~ 25 % and ~ 30% respectively.

Keywords : Microstructure, Magnesium, Hardness, Tensile properties, Ageing, Casting

1. INTRODUCTION

Among all the metals, magnesium is the lightest metal known on earth used for structural applications and also Magnesium is easily available [1]. Mg-Al series and Mg-Zn series, such as AZ91, AM60, AM40, ZK61 etc. are most popularly utilized Mg alloys [2-3]. A combination of properties such as high specific strength, high specific modulus, heat dissipation, weldability, high damping, etc. makes Mg alloy as a potential material for various applications like in aerospace and automobile [4-5]. It also shows excellent castability and can be cast by most conventional methods. Thus, Mg alloys are considered to be a better choice for high-temperature applications in the future. The most frequently used alloy for automotive applications is die-cast AZ91 alloys which shows an excellent mechanical properties at ambient temperature. However, the properties start to deteriorate relatively at higher temperatures (i.e) ~ above 120°C [6]. The presence of a stable room temperature $Mg_{17}Al_{12}$ secondary phase in AZ91 alloy contributes to excellent mechanical property at ambient conditions. However, owing to the lower melting point of $Mg_{17}Al_{12}$ intermetallic phase (437°C), it becomes highly unstable at elevated temperatures which leads to poor creep resistance. Therefore, Mg alloys containing Al and Zn as major alloying elements are not suitable for a component that operates at high temperatures. Moreover, the introduction of rare earth metal improves the mechanical properties of such Mg alloys for high-temperature applications but these are highly expensive materials and it also increases the density of the alloy [7]. In recent years, attempt is made to replace a conventional Mg alloys for elevated temperature applications, Mg-Sn alloy has been shown a great potential among all other alloy system.

In the last two decades, Mg-Sn system has gained much attention due to their better creep resistance properties [8-10]. These alloys are cheaper and can also be strengthened through age hardening. Owing to the drastic decline in solubility of Sn in Mg matrix with lowering the temperature, Mg-Sn system shows excellent effects on tensile properties during aging [11-13]. The binary phase diagram of Mg-Sn shows that the solid solubility of Sn decreases from ~14wt.% at 561°C (eutectic transformation temperature) to less than 0.5wt.% at room temperature [14]. The addition of Zn and Al promotes the age-hardening response of Mg-Sn alloy [11]. It has been reported

Corresponding Author.
E-mail : ppoddar3@gmail.com

that the Mg-Sn alloy system shows excellent creep resistance at an elevated temperature according to the findings of a study conducted by H. Liu et al. [15]. It has been shown that Mg-10Sn (wt%) binary system exhibit creeps property better than AE42 alloy. The former system is consisting of Mg_2Sn secondary phase which is a thermally stable phase with a melting point of 770˚C. The stable microstructures at high temperatures are often produced as a result of a stable Mg_2Sn secondary phase. Moreover, the presence of Mg_2Sn precipitates hinders the movement of grain boundary by pinning it down, thereby, creep resistance improved significantly. In addition, Mg_2Sn phase is also known to be hard and brittle. As a result, the strength of the alloy can be enhanced. According to S. Wei al, the tensile strength of AZ62 increases with the addition of Sn [16].

Although Mg-10Sn (wt%) alloy has shown excellent creep properties, a limited research has been done to explore the effects of alloying elements and ageing on its mechanical properties. In this study, the emphasis has been given on microstructural development of different Mg-Sn alloys in as-cast and aged condition, and mechanical properties are correlated to the corresponding alloy system. Moreover, the comparative study will demonstrate the role of alloying elements (Al and Zn) on microstructures and mechanical properties of Mg-Sn alloy. Mg-10Sn (wt%) (T10) binary alloy, Mg-10Sn-3Al (wt%) (TA103) and Mg-10Sn-3Al-1Zn (wt%) (TAZ1031) are chosen to investigate on the above mentioned aspects.

2. EXPERIMENTAL PROCEDURE

T10, TA103 and TAZ1031 and Alloys were prepared by melting the commercial Mg (purity: 99.85%), Sn (purity: 99.99%), Al (purity: 99.96%) and Zn (purity: 99.99%) at 770°C . Castings with a dimension of 30 X 18 X 2 (cm) were prepared using a steel crucible after melting. The temperature of furnace was first maintained at approx. 770˚C and each ingot was preheated at around 150˚C. After the crucible was heated, the preheated Mg ingots were charged into the crucible. Initially, the Mg ingots were melted completely, then, the rest of the ingots were introduced into the melt. During melting, the top surface of the melt was covered with the flux and uninterrupted supply of argon was provided to prevent the oxidation of the melt which is explosive in nature. After reaching the temperature of 770˚C, the melt was held at this temperature to ensure uniform and complete melting. The melt was then poured into a preheated (at 250˚C) mould of cast iron with passing the argon gas around the melt and kept it at room temperature to solidify.

Casting from each alloy was solution-treated at 400˚C for 1h, followed by water quenching. During solution treatment, the blocks were kept in a cast iron container, covered with sand and in an atmosphere continuously supplied with Argon gas to avoid the contact of air with casting blocks. This arrangement is to prevent the risk of oxidation of casting blocks. The castings were subsequently aged at 200˚C for 100 hr and 500 hr. For microstructure analysis, samples of as-cast and aged samples of each alloy were polished upto 4000 grid paper followed by cloth polishing. Samples were finally etched for 7 to 10 sec in 2% Nital solution and washed with ethanol. Microstructural images with different magnifications were taken under an optical microscope and scanning electron microscope fitted with an energy dispersive spectroscopic analyzer. The phases were identified using X-ray diffraction technique. Cu-K_α radiation (λ = 1.5418 Å) was used in the X-ray diffractometer. The characteristic peaks of different phases were identified using a commercial software EVA. The hardness was measured for as-cast and aged alloys by using Vicker'shardness testing machine at constant load of 25g with a dwell time of 10 sec. Ten readings were taken from each sample to obtain a statistically reliable hardness value. Tensile tests were performed in a servo-electric test machine at a cross-head speed of 0.03mm/sec at room temperature in accordance with ASTM E8-13a standard. The gauge length and its cross section of tensile specimen were 30mm and 6mm X 6 mm respectively. The fracture surface of the tensile-tested samples was investigated under SEM.

3. RESULT AND DISCUSSION

3.1. Microstructural Characterization

3.1.1. As cast material

Optical microstructures of as cast studied alloys (T10, TA103 and TAZ1031) are shown in Fig.1 (a-c). Microstructure of as cast binary alloy Mg-10Sn (wt%) is consisting of two phases, primary Mg and Mg_2Sn secondary phase as shown by XRD spectrum in Fig. 2 (a). Optical image of Mg-10Sn (wt%) in Fig. 1 (a) displays a dendritic structure where light region shows the matrix (primary α Mg: solid solution of Sn in Mg) and dark region shows Sn rich eutectic phase as Sn rich area etch faster as compare to Mg matrix. The eutectic phase of α Mg + Mg_2Sn, which was formed during the later stage of solidification of melt, is present at inter-dendritic spacing and forming a semi-continuous network. The dendrite structure of Mg-Sn alloy depends upon solidification parameters, like cooling rate and alloy composition, and the volume fraction of Mg_2Sn phase increases with increase in quantity of Sn added in the alloy [17-18]. In as cast TA103 alloy is consisting of three phases as shown in Fig. 2(b). The presence of 3wt.%Al rises to an additional phase, $Mg_{17}Al_{12}$ intermetallic phase. While 1 wt.%Zn doesn't contribute to the formation of any other precipitate but enhances the precipitation process for other secondary phases in TAZ1031. The area percentage of precipitate for TAZ1031 (5.6%) is higher than that of TA103 (4.7%). SEM-EDS micrograph of as TA103 and TAZ1031 shown in Fig. 8 (a) and Fig. 9 (a) respectively indicate the presence of Mg_2Sn and $Mg_{17}Al_{12}$ intermetallic phase at grain boundaries. As compared to binary alloy, the microstructure of TA103 and TAZ1031 alloys has higher number of discrete precipitates within the grain.

3.1.2 Heat Treated Material

The solution treatment of as-cast materials was done at 400°C, keeping the safest common temperature for all the composition under consideration. Ageing was conducted at 200°C for period of 100hr and 500hr. It has been reported that the time to reach the peak hardness on aging in Mg-Sn alloy is minimum at 200°C [19-20]. Therefore, the aging temperature of 200 °C has been chosen for the study. Owing to the fact that the slow diffusion of Sn atoms in Mg matrix renders ageing a sluggish process for Mg alloy, time to reach peak hardness is more than 100 hr, thus the aging duration of 100 hr and 500 hr was chosen for this investigation. Similar findings on ageing of a Mg-Sn-Al-Zn alloy system were reported by T.T Sasaki et al. [21]. The microstructural variations during the ageing treatment at 200°C have been recorded in all alloy samples using scanning electron microscopy along with EDS and optical microscopy. Mg-Sn alloys shows good age hardening response because of the declining solid state solubility of Sn in magnesium with temperature makes. The maximum solid state solubility of Sn in Mg is around 14.48 wt.% at 561°C which drop down to less than 1 wt. % at room temperature. During solution treatment, alloying element dissolves into the matrix which forms a supersaturated solid solution after quenching. The alloying elements start to diffuse held at 200°C and form fine precipitates of intermetallic compound which is distributed throughout the matrix and causes precipitation hardening according to Orowan mechanism [22]. Aging has also promoted fine recrystallized grains structure.

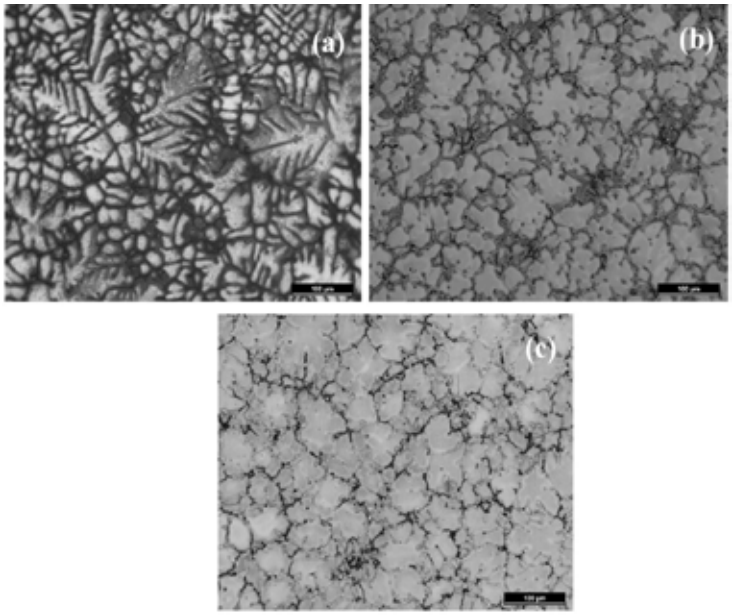

Fig.1: Optical micrograph of as cast (a) T10 (b) TA103 and (c) TAZ1031 alloys

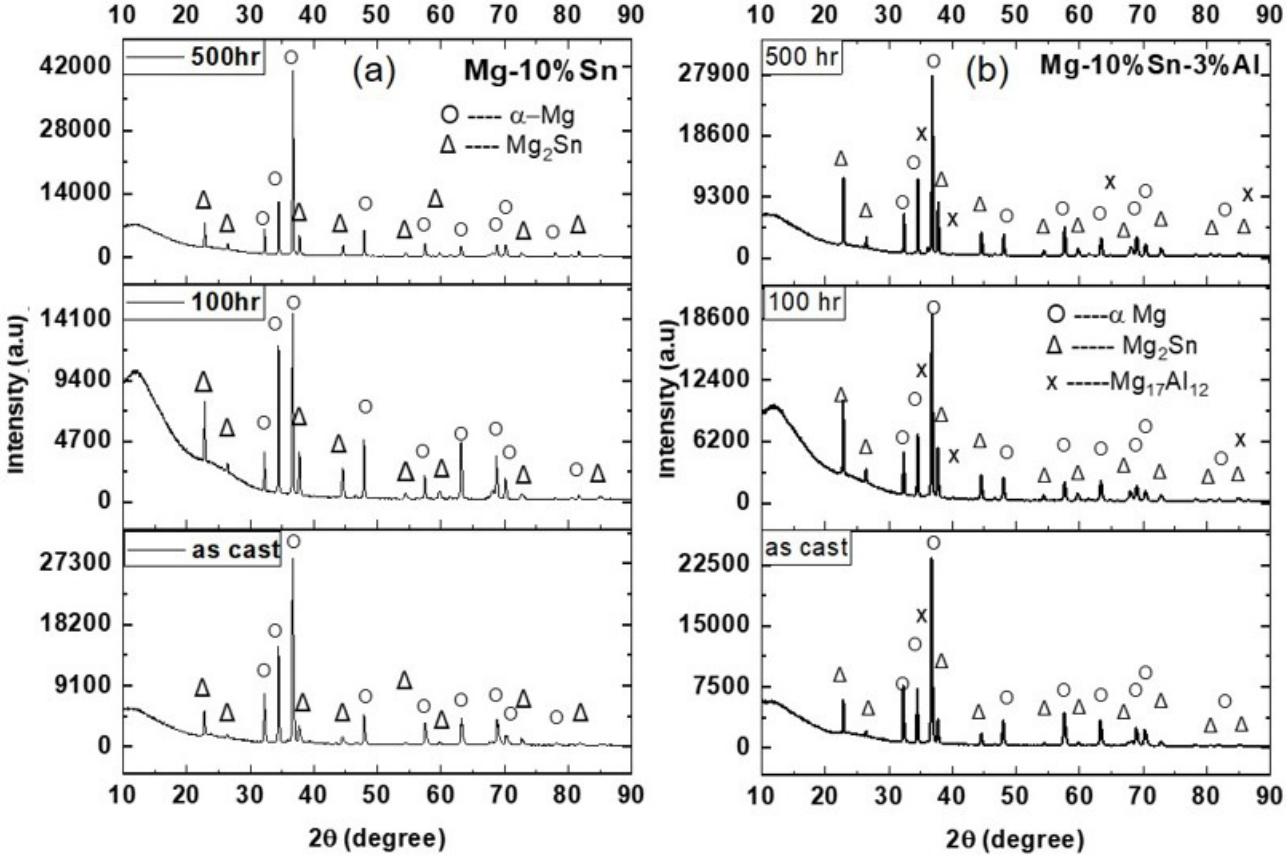

Fig.2 : XRD spectrum of (a) Mg-10Sn (wt%), (b) Mg-10Sn-3Al (wt%) alloys at different heat treated conditions

Scanning electron micrographs and optical image of as-cast Mg-10Sn (wt%) alloy shown in Fig. 4 (a) and 3 (a) respectively has shown that the major amount of intermetallic phase is present along the grain boundaries discontinuously. Very small amounts of such intermetallic particles are found to be present within the grain in the as-cast alloy. On the other hand, after ageing Mg_2Sn precipitates have formed within the grain in small quantity shown in Fig. 5 (a). Similar finding was presented by G. Nayyeri et al. in his study on Mg-5Sn (wt%) showing that the particles of Mg_2Sn get distributed within grains after ageing at 200˚C [23]. The primary Mg_2Sn precipitate present in as-cast alloy is not able to dissolve entirely in the α-Mg matrix during solution treatment due to sluggish diffusion of Sn leading to slow dissolution of the phase. Therefore, some primary Mg_2Sn precipitates, reduced in size, are still present along the grain boundaries post ageing. Optical images in Fig. 5 and 6 illustrates the microstructure of TA103 and TAZ1031 after 100hr of ageing and SEM images in Fig. 4illustrates the microstructure of as cast and aged Mg-10Sn (wt%) at 100hr and 500 hr conditions. It depicts that the precipitates of Mg_2Sn and $Mg_{17}Al_{12}$ intermetallic phases are distributed throughout the matrix of TA103 and TAZ1031 after ageing. The presence of secondary phases in T10 alloy, identified as Mg_2Sn phase, is shown in Fig 7. SEM-EDS micrograph in Fig.8 shows the microstructural features with composition, corroborating the presence of these two secondary phases. Introduction of Al increased the amount of precipitate formation during ageing because adding 3% Al improved the dissolution of secondary phase into the matrix during solution treatment. No Mg-Zn or Mg-Al-Zn intermetallic phase was found by adding 1% Zn but according to N. El Mahallawy, it cause coarsening of Mg_2Sn precipitates in Mg-Sn-Zn alloy [24]. Fig. 9 shows the SEM-EDS micrographs of as cast Mg-10Sn-3Al-1Zn (wt%) and aged Mg-10Sn-3Al-1Zn (wt%) alloy after 100 hr of holding time at 200˚C. These alloys, especially at heat treated conditions, the Mg_2Sn, and $Mg_{17}Al_{12}$ phases are clearly identified.

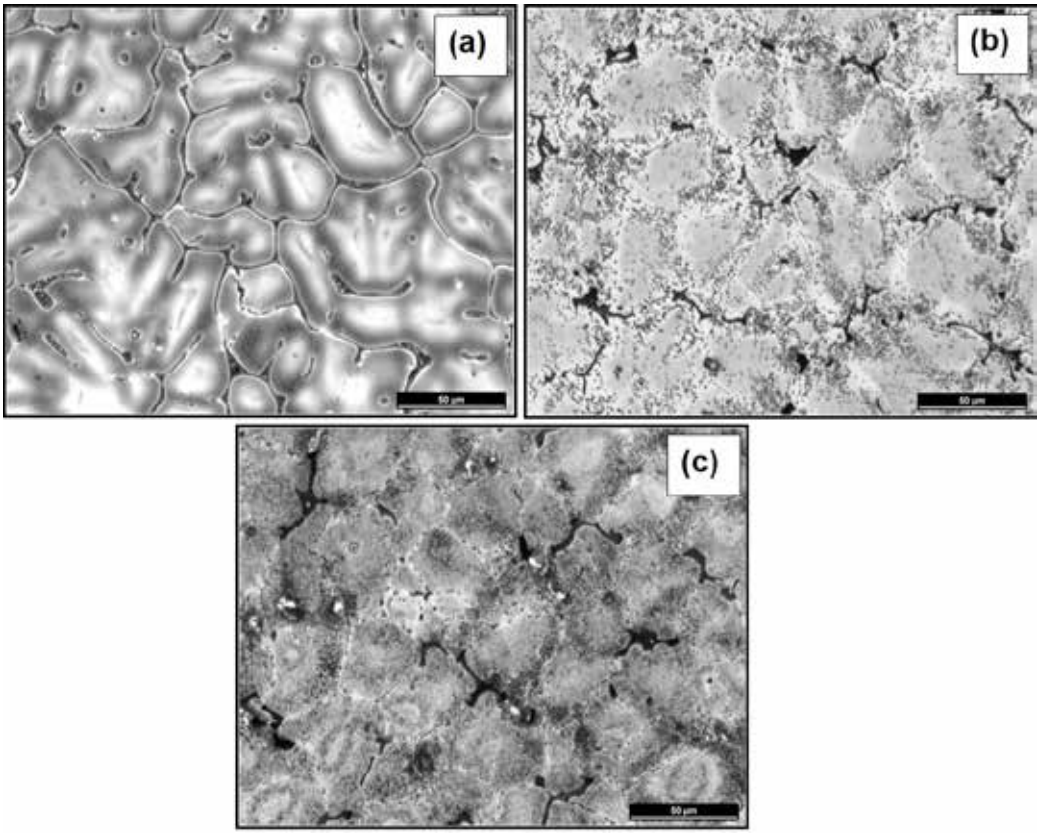

Fig.3: Optical microstructures of (a) Mg-10Sn (wt%), (b) Mg-10Sn-3Al (wt%) and (c) Mg-10Sn-3Al-1Zn (wt%) after 100hr of holding time at 200˚C

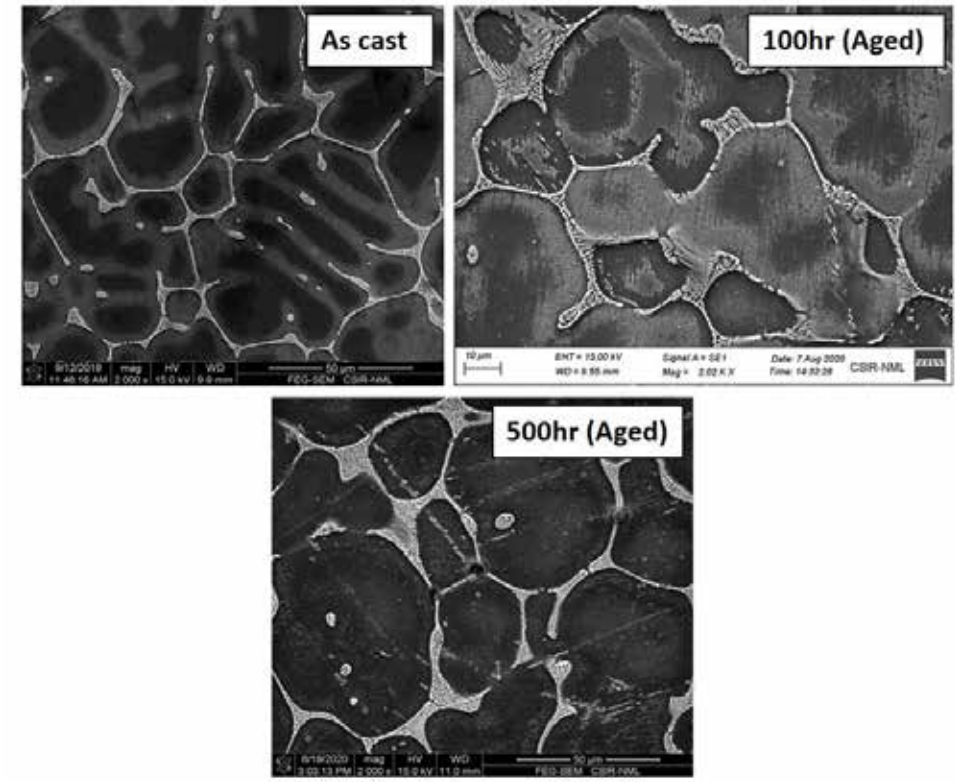

Fig. 4: Scanning electron microscopic images of Mg-10Sn (wt%) alloy at as cast and different ageing condition

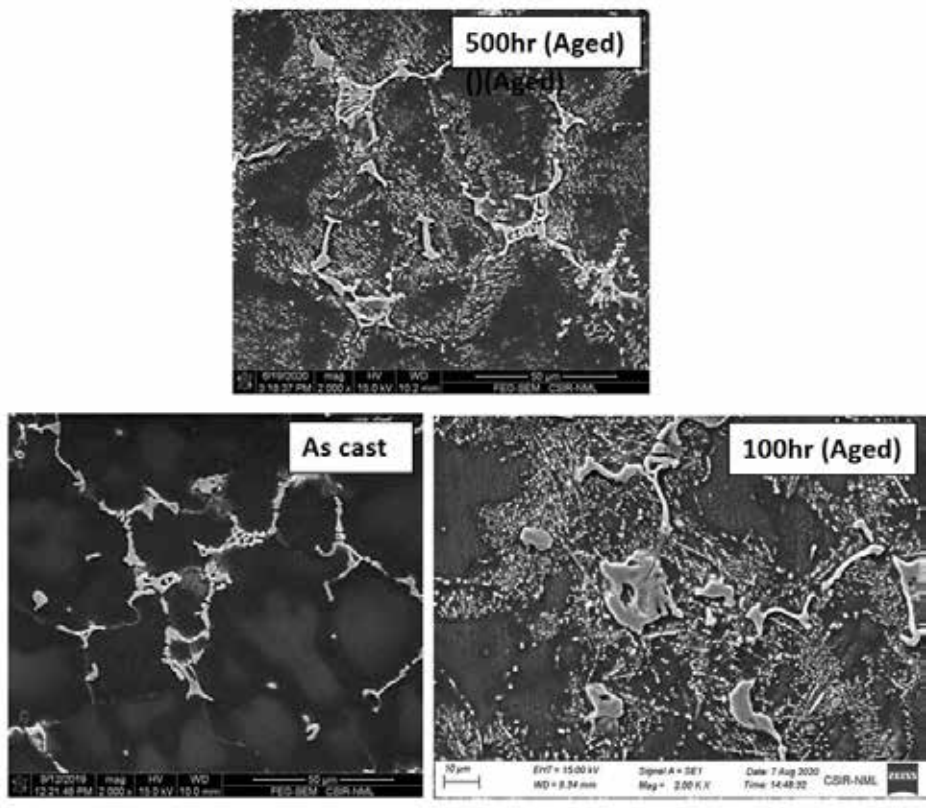

Fig. 5: Scanning electron microscopic images of Mg-10Sn-3Al (wt%) alloy at as cast and different ageing condition

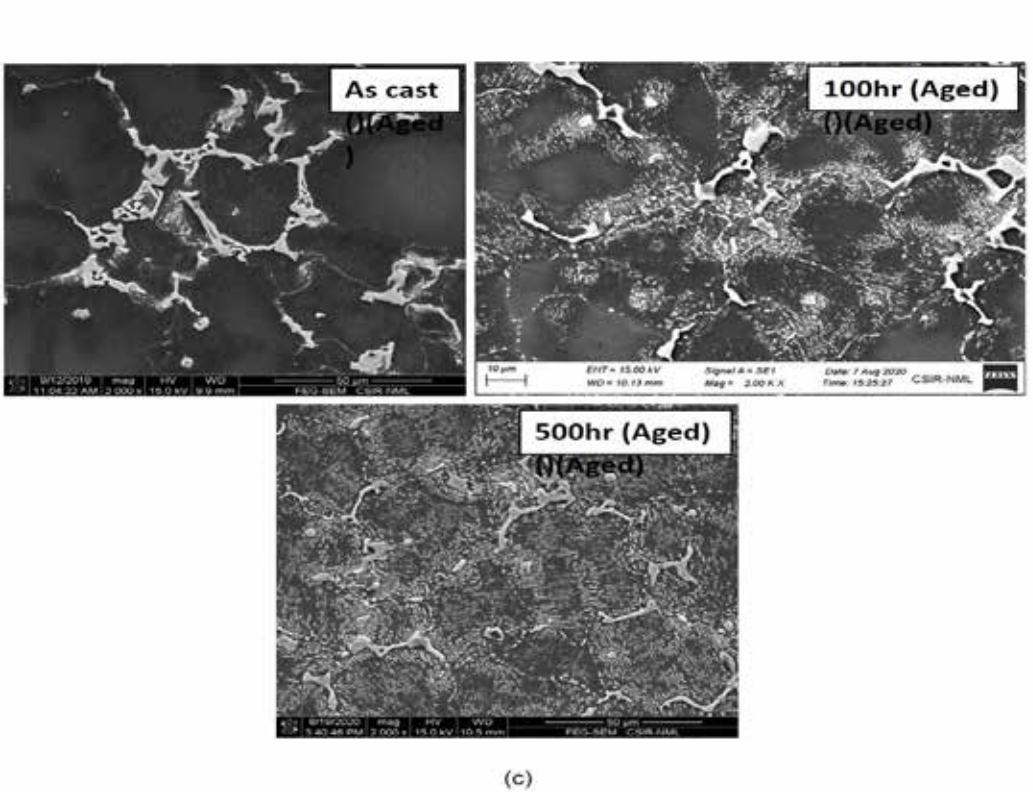

Fig. 6: Scanning electron microscopic images of Mg-10Sn-3Al-1Zn (wt%) alloy at as cast and different ageing condition

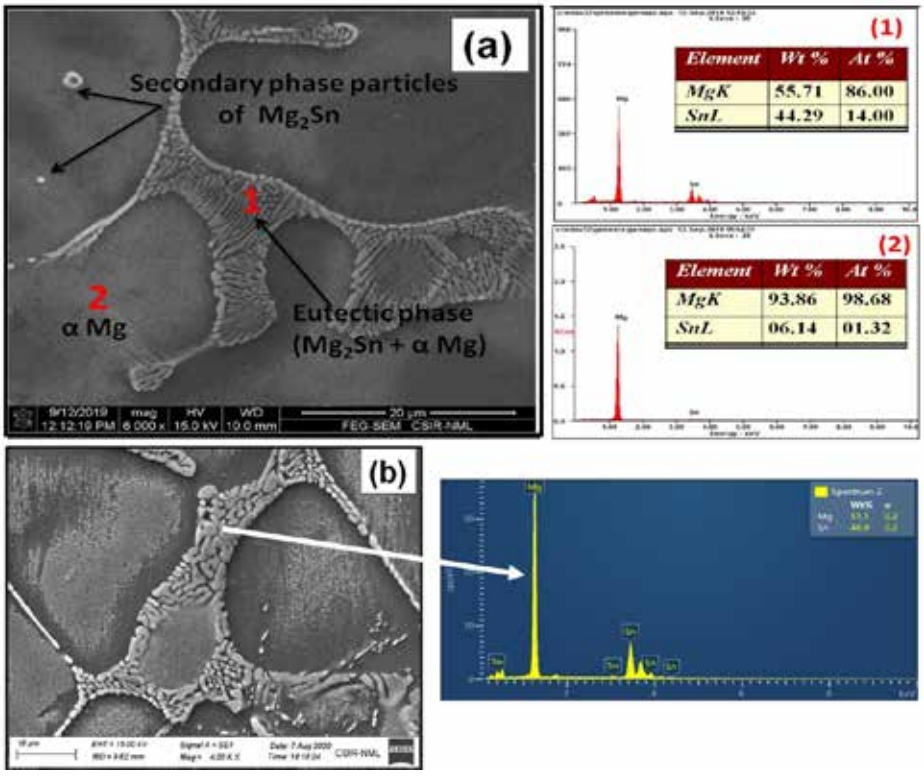

Fig. 7: SEM-EDS micrographs of (a) as cast Mg-10Sn (wt%) (b) aged Mg-10Sn (wt%) after 100 hr of holding time at 200°C

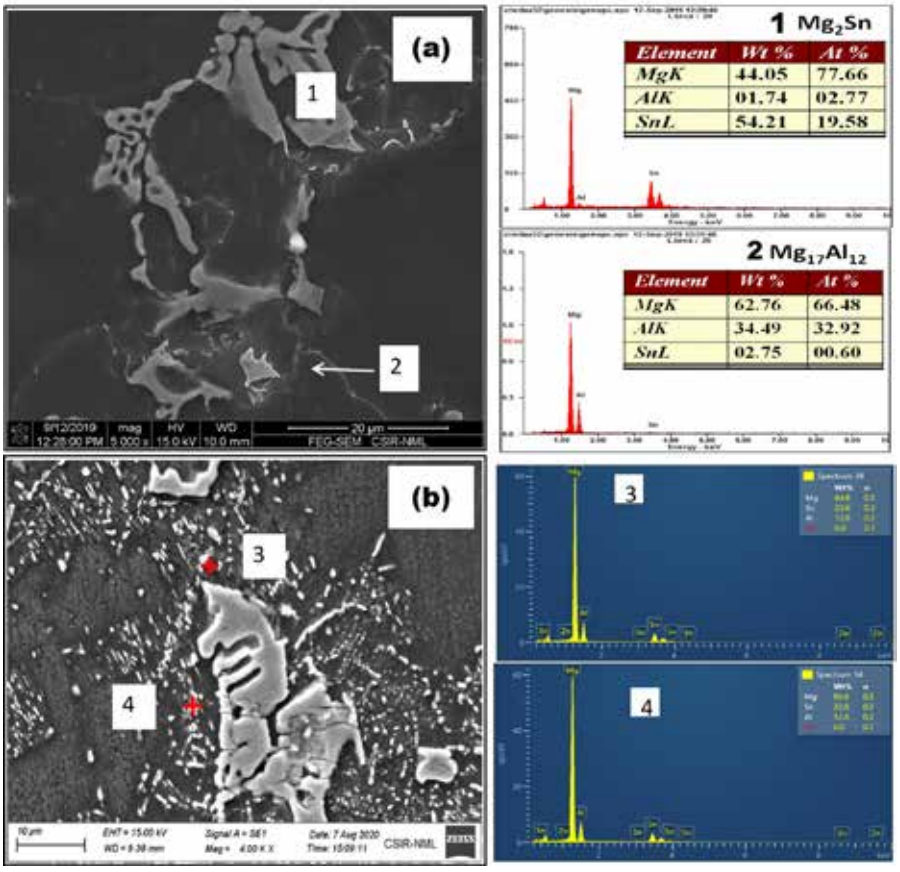

Fig. 8: SEM-EDS micrographs of (a) as cast Mg-10Sn-3Al (wt%) (b) aged Mg-10Sn-3Al (wt%) after 100 hr of holding time at 200°C

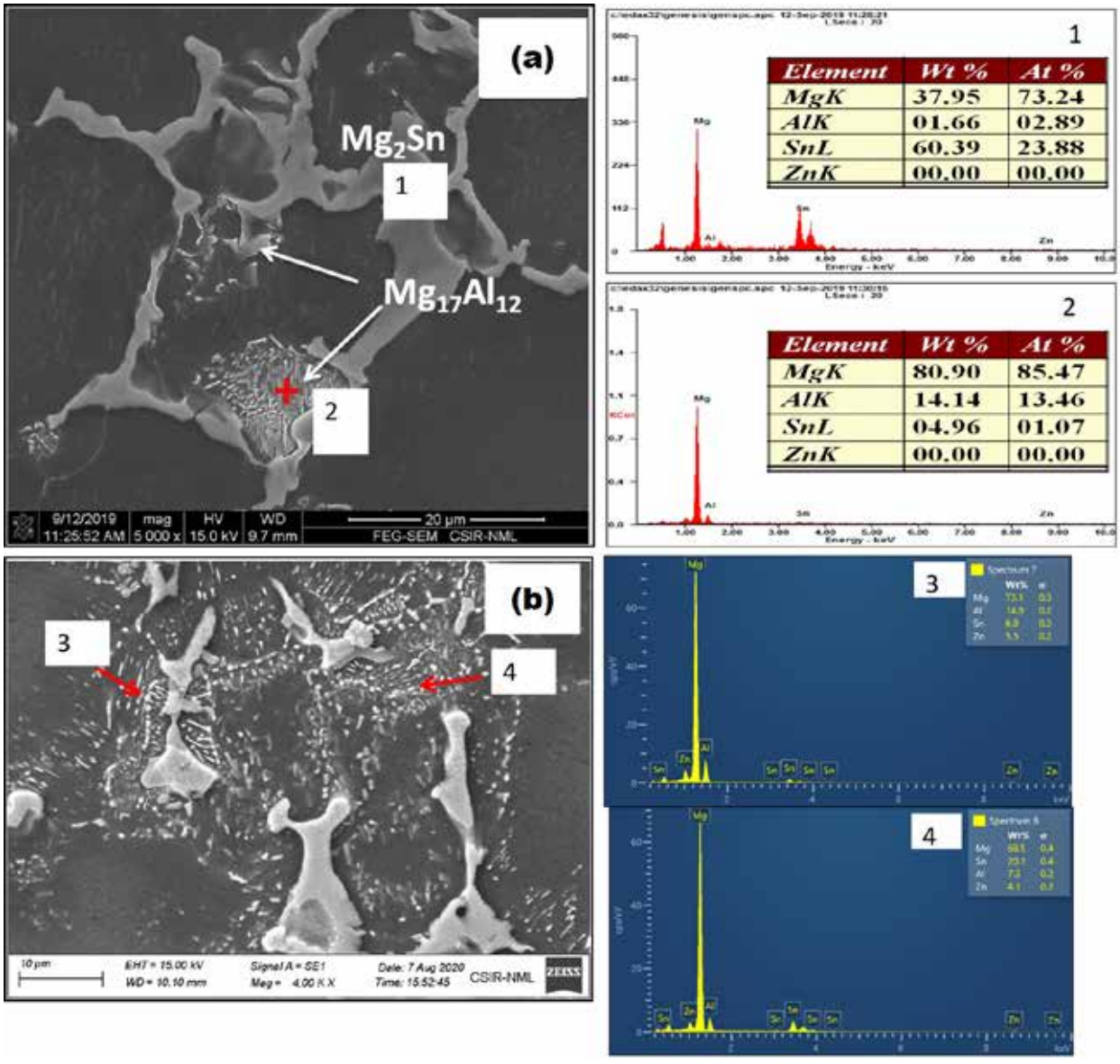

Fig. 9: SEM-EDS micrographs of (a) as cast Mg-10Sn-3Al-1Zn (wt%) (b) aged Mg-10Sn-3Al-1Zn (wt%) after 100 hr of holding time at 200°C

3.2. MECHANICAL PROPERTY EVALUATION

3.2.1. Hardness Measurement

Grain refinement, solid solution hardening and precipitate hardening are the major hardening and strengthening mechanisms that are found in Mg alloy. Fine grain materials show better strength and hardness properties than material with coarse grain structure. According to the Hall-Petch equation ($\Delta\sigma_n = kd^{-1/2}$, where d is the average grain size ranging from ~26 to ~32 µm and k is constant) grain refinement gives better hardness and yield strength [25]. Further more, the addition of alloying elements gave rise to grain refinement and hence improved hardness of as cast TA10 and TAZ 1031 alloy (Fig 10). Alloying elements play an imperative role in grain refinement. The segregation of alloying elements at solid/liquid interface instigates constitutional super cooling that promotes the nucleation of new grains and restricts the growth of primary grains [26]. The influence of Constitutional super cooling can be expressed by GRF (Grain Restriction Factor also called Q-value). $Q = m C_o (k-1)$ where m represents the slope of the liquidus line, C_o represents initial composition of the alloy and k represents equilibrium partition coefficient for element [27-28]. Grain size of as cast T10, TA103 and TAZ1031 is 102 µm, 65 µm and

58 µm respectively (Fig 11). With the addition of 3% Al, grain size has dropped drastically which contributed for the higher hardness of TA103 (52 HV) than T10 (41 HV). Moreover, incorporation of 1% Zn further reduced the grain size of as cast TA103, resulting in slight improvement in hardness with the value of 54 HV. There is no evidence of any intermetallic compound containing Zn element which suggest that Zn atoms are dissolved in the Mg-matrix contributing to the solid solution strengthening.

Variation in hardness, grain size and area fraction of precipitates of different materials with ageing time is illustrated in Fig. 10, 11 and 12 respectively. By comparing these three graphs, it is clearly identified the effect of grain size and area fraction on the hardness property of alloys. Lower grain size and higher area fraction resulted in better hardness value. Mg-10Sn (wt%) alloy showed very little increment in hardness value after ageing for 100 hr and 500 hr. while, it also exhibited very little raise in area fraction and reduction in grain size, which subsequently could be a reason for the minimal hike in hardness value of T10 alloy after ageing. Moving forward to TA103, after ageing for 100 hr the grain size dropped by 35% and area fraction of the secondary phase increased significantly from 5.8% to 26%. It consequently boosted hardness by 25%, where after 500 hr, a slight reduction in the hardness value was recorded because the grain size of TA103 remained more or less the same and the area fraction dropped from 26% to 19%. Similarly in case of TAZ1031, the hardness value increased after both 100 hr and 500 hr of ageing time due consistent grain refinement and increment of area fraction.

There could be three major mechanisms behind the improved hardness value of alloy with Al addition. First of all, introduction of aluminum lowers the solid solubility of Sn, hence booster the driving force for the precipitation. Secondly, the presence of $Mg_{17}Al_{12}$ precipitates that probably acted as nucleation sites for the formation of hard Mg_2Sn intermetallic phase and increased the amount of secondary phase and last one is grain refinement. A study conducted by F.R. Elsayed et.al., suggested that adding Al in Mg-Sn system not only increases the quantity of intermetallic phase but also refines the precipitates. Additional incorporation of Zn further reduces the size of the precipitates and thereby improves on precipitation hardening [11].

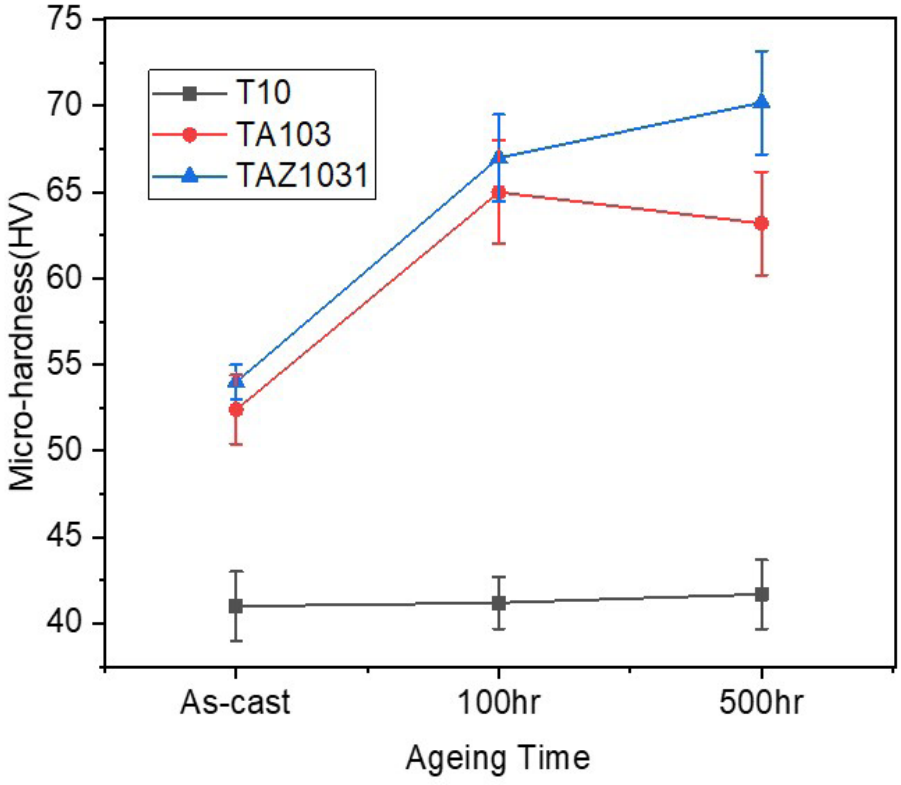

Fig. 10: The graphical representation of micro-hardness at different heat treatment condition

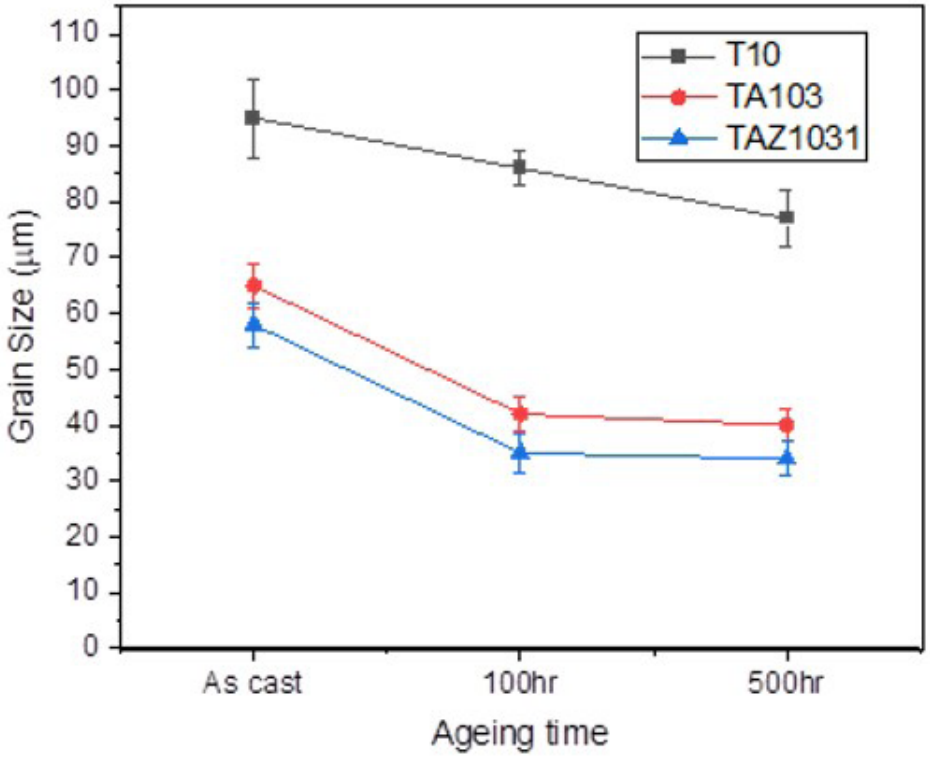

Fig. 11: The graphical representation of grain size at different heat treatment condition

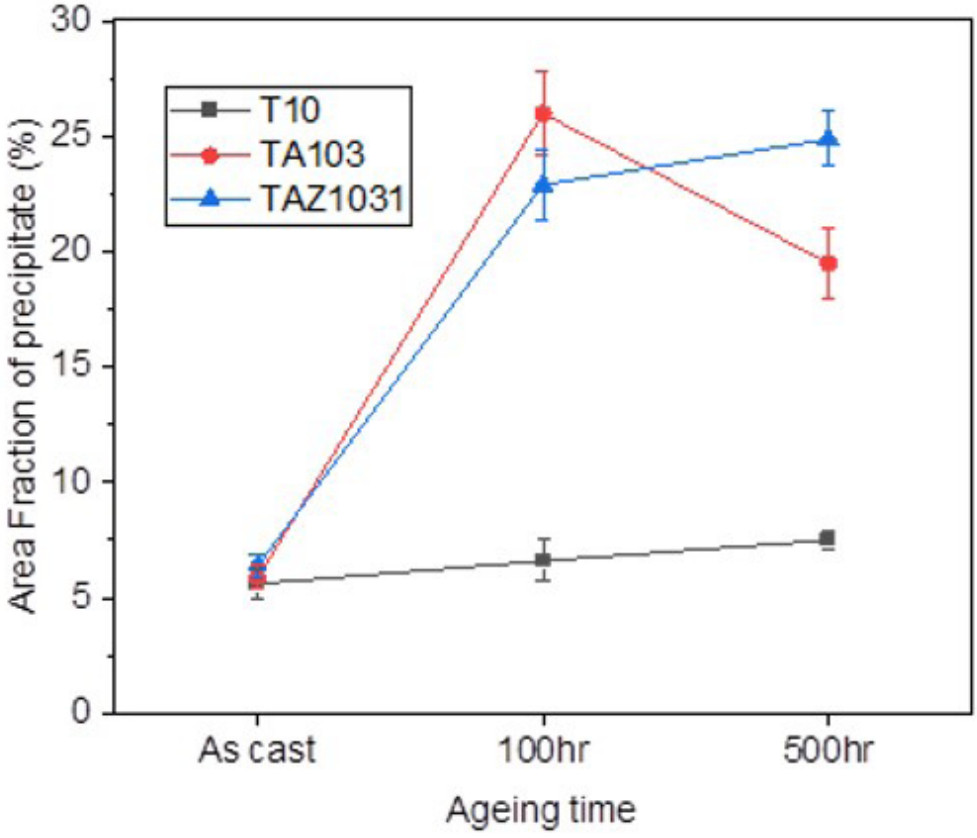

Fig. 12: The graphical representation of area fraction of the precipitates (secondary phase) at different heat treatment condition

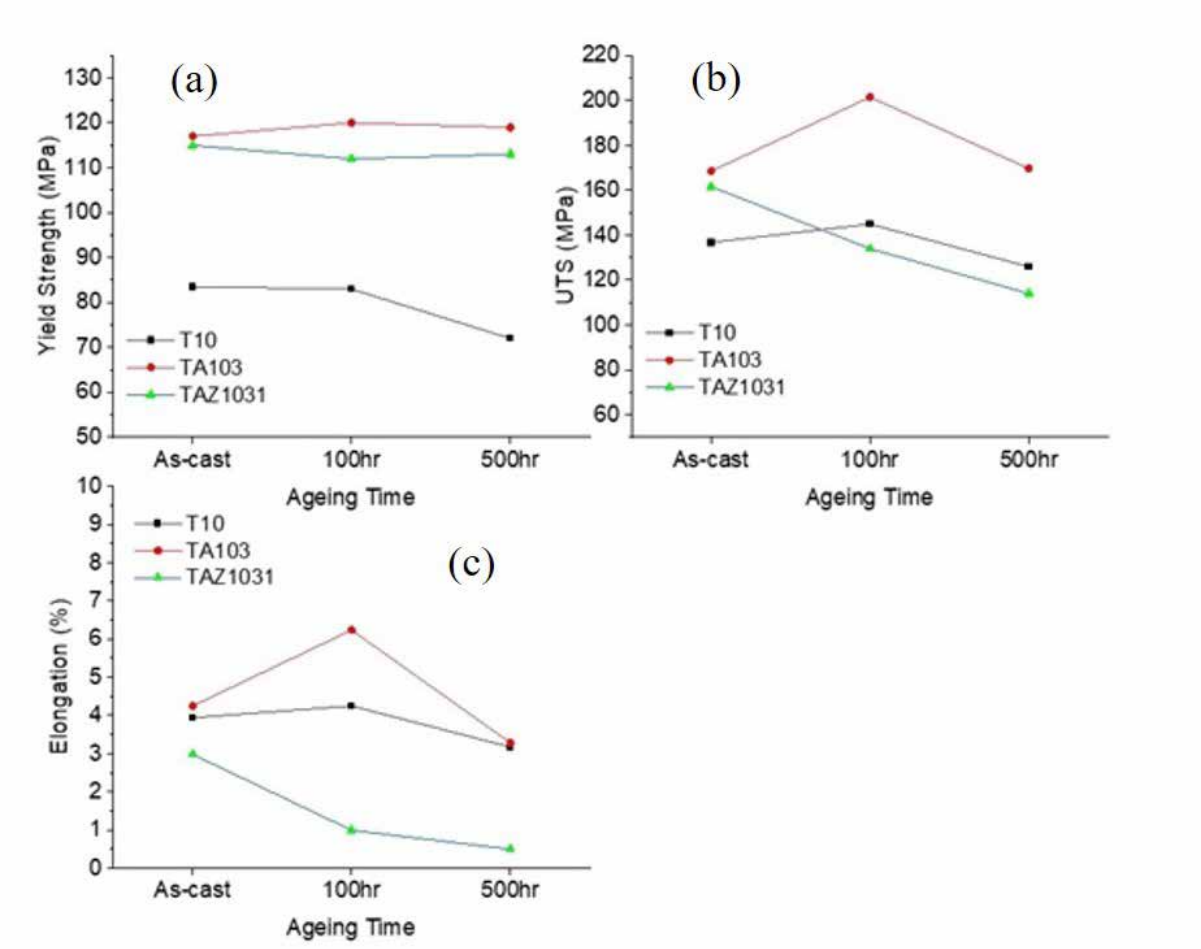

Fig. 13: Graphical representation of variation of (a) yield strength (YS), (b) ultimate tensile strength (UTS) and (c) % elongation of each alloy with holding time at 200˚C

3.2.2 Tensile properties and fractography

Fig. 13 shows the graphical representation of variation of (a) yield strength (YS), (b) ultimate tensile strength (UTS) and (c) % elongation of each alloy with holding time at 200˚C. Mg-10 Sn-3Al (wt%) shows YS, UTS and % elongation values of 120 MPa, 201 MPa and 60.23% respectively. As compare to as cast condition, aged Mg-10Sn-3Al (wt%) and Mg-10Sn-3Al -1Zn (wt%) exhibited higher hardness value by ~ 25 % and ~ 30% respectively. Fig.14 shows the fracture morphology of tensile specimens after testing. Owing to the limited ductility of as cast Mg-Sn at room temperature due to restricted number of slip systems [2-3], they are brittle in nature. In case of Mg-10Sn (wt%), the presence of flat facets and very little flow of material in the stretching direction is indicative of its brittleness. Similarly after ageing, there is no significant evidence of considerable amount of plastic deformation, also, the presence of ridges exhibits cleavage mode of fracture. Micrographs of TA103 alloy in Fig. 14 shows small and not so deep dimples implying the occurrence of slight amount of plastic deformation prior to failure. On the other hand, the fracture surfaces of TAZ1031 (Fig. 14) alloys has granular appearance and numerous cracks. In fact after ageing the fractured surface displays many cracks and flat facets throughout the microstructure that suggests the extremely high brittleness of the material. Fractography images also show the intergranular brittle fracture of the samples which can be credited to the presence of coarse secondary phase particles at the grain boundary. Crack initiations take place at the precipitate matrix interface and propagate along the grain boundary. Ultimately, it results in fracture and produces cavities on the fracture surface due to the extraction of grains.

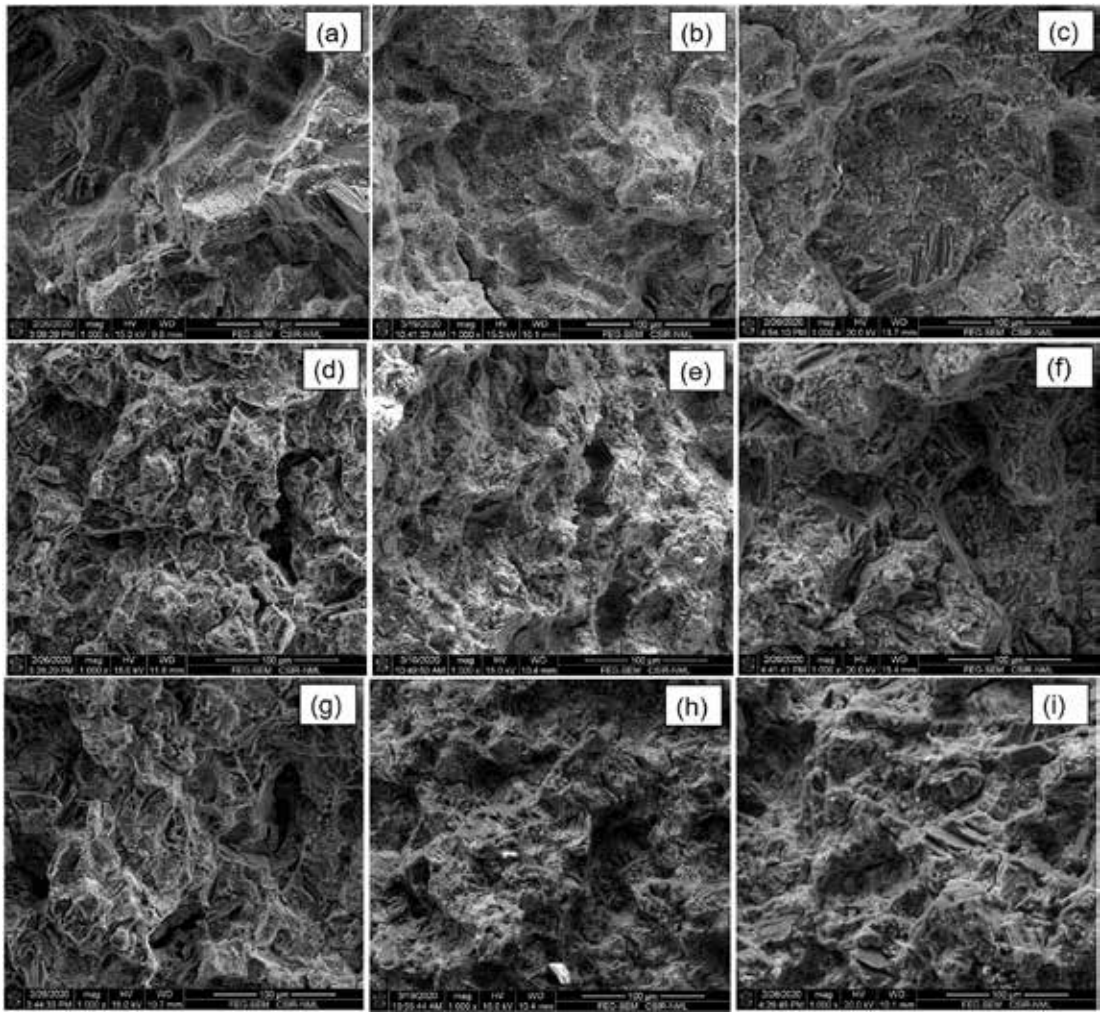

Fig. 14. SEM images of fracture surface of as cast (a) T10 (d) TA103 and (g) TAZ1031 (b, e, h) fracture surface of aged (100hr) T10, TA103 and TAZ1031 respectively. (c, f, i) fracture surface of aged (500hr) T10, TA103 and TAZ1031 respectively.

4. **CONCLUSION**

1. Mg-10Sn (wt%) alloy consist of only one kind of intermetallic phase i.e. Mg_2Sn. Addition of 3% Al resulted in formation of $Mg_{17}Al_{12}$ secondary phase. On the other hand, further addition of 1% Zn doesn't form any new intermetallic compound. However, it increases the amount of secondary phase precipitates.
2. Addition of Al and Zn causes grain refinement due to segregation of alloying elements at liquid/ solid interface which restricts the grain growth. Among all as cast alloys, TAZ1031 has the finest grains.
3. Addition of Al and Zn increases the hardness of Mg-10Sn (wt%) binary alloy due to solid solution strengthening and grain refinement. It also enhances the age hardening response of Mg-Sn alloy. TAZ1031 alloy after 500 hr of ageing at 200^{o}C exhibited the highest value of hardness.

5. **REFERENCES**

1. W. Jia, Q. Le : Heat-transfer analysis of AZ31B Mg alloys during single-pass flat rolling : Experimental verification and mathematical modeling, Materials Design, 121, 288-309, 2017.
2. S. T. E. M Celotto : TEM study of continuous precipitation in Mg–9 wt% Al–1 wt% Zn alloy. Acta materialia, 48(8), 1775-1787, 2000.
3. I. J. Polmear : Magnesium alloys and applications. Materials science and technology, 10(1), 1-16, 1994.

4. T Mukai, M Yamanoi, H Watanabe: Ductility enhancement in AZ31 magnesium alloy by controlling its grain structure. Scripta materialia, 45(1), 89-94, 2001.
5. H. Hu, A. Yu, N. Li, J. E. Allison: Potential magnesium alloys for high temperature die cast automotive applications: a review. Materials and Manufacturing Processes, 18(5), 687-717, 2003.
6. J. G. Wang, L. M. Hsiung, T. G. Nieh, M. Mabuchi: Creep of a heat treated Mg–4Y–3RE alloy. Materials Science and Engineering: A, 315(1-2), 81-88, 2001.
7. G. Pettersen, H. Westengen, R. Høier, O. Lohne : Microstructure of a pressure die cast magnesium—4wt.% aluminium alloy modified with rare earth additions. Materials Science and Engineering: A, 207(1), 115-120, 1996.
8. A. L. Bowles, H. Dieringa, C. Blawert, N. Hort, K. U. Kainer: Investigations in the Magnesium-Tin system. In Materials Science Forum, Vol. 488, 135-138, 2005.
9. H. Sevik, S. Açıkgöz, S. C. Kurnaz : The effect of tin addition on the microstructure and mechanical properties of squeeze cast AM60 alloy. Journal of Alloys and Compounds, 508(1), 110-114, 2010.
10. D. H.Kang, S. S. Park, & N. J. Kim: Development of creep resistant die cast Mg-Sn-Al-Si alloy. Materials Science and Engineering A, 413–414, 555–560, 2005.
11. F. R. Elsayed, T. T. Sasaki, C. L. Mendis, T. Ohkubo, K. Hono: Compositional optimization of Mg-Sn-Al alloys for higher age hardening response. Materials Science and Engineering A, 566, 22–29, 2013.
12. T. T. Sasaki, K. Oh-ishi, T. Ohkubo, K. Hono : Effect of double aging and microalloying on the age hardening behavior of a Mg-Sn-Zn alloy. Materials Science and Engineering A, 530(1), 1–8, 2011.
13. P. Poddar, A. Kamaraj, A. P. Murugesan, S. Bagui, K. L. Sahoo: Microstructural features of Mg-8%Sn alloy and its correlation with mechanical properties. Journal of Magnesium and Alloys, 5(3), 348–354, 2017.
14. H. Okamoto, T. B. Massalski : Binary alloy phase diagrams. ASM International, Materials Park, OH, USA, 1990.
15. H. Liu, Y. Chen, Y. Tang, S. Wei, G. Niu : The microstructure, tensile properties, and creep behavior of as-cast Mg-(1-10)%Sn alloys. Journal of Alloys and Compounds, 440(1–2), 122–126, 2007.
16. S.Wei, Y. Chen, Y. Tang, H. Liu, S. Xiao, G. Niu, X. Zhang, Y. Zhao : Compressive creep behavior of as-cast and aging-treated Mg-5 wt% Sn alloys. Materials Science and Engineering A, 492(1–2), 20–23, 2008.
17. F. Yavari, S. G. Shabestari : Effect of cooling rate and Al content on solidification characteristics of AZ magnesium alloys using cooling curve thermal analysis. Journal of Thermal Analysis and Calorimetry, 129(2), 655-662, 2017.
18. X. Cui, W. Yuying, L. Xiangfa: Microstructural Characterization and Mechanical Properties of VB2/A390 Composite Alloy, Journal of Materials Science and Technology 31(10), 1027–1033, 2015.
19. T.T Sasaki, K. Oh-ishi, T. Ohkubo, K. Hono: Effect of double aging and micro alloying on the age hardening behavior of a Mg–Sn–Zn alloy, Materials Science and Engineering A 530, 1-8, 2011.
20. A. E. Davis, J. D. Robson, M. Turski: The effect of multiple precipitate types and texture on yield asymmetry in Mg-Sn-Zn(-Al-Na-Ca) alloys. Acta Materialia, 158, 1–12, 2018.
21. T. T. Sasaki, F. R. Elsayed, T. Nakata, T. Ohkubo, S. Kamado, K. Hono: Strong and ductile heat-treatable Mg–Sn–Zn–Al wrought alloys. Acta Materialia, 99, 176-186, 2015.
22. C. L. Mendis, K. Hono : Understanding precipitation processes in magnesium alloys, In Fundamentals of Magnesium Alloy Metallurgy: A volume in Woodhead Publishing Series in Metals and Surface Engineering, Woodhead Publishing Limited, 2013.
23. G. Nayyeri, R. Mahmudi, F. Salehi : The microstructure, creep resistance, and high-temperature mechanical properties of Mg-5Sn alloy with Ca and Sb additions, and aging treatment. Materials Science and Engineering: A, 527(21-22), 5353-5359, 2010.
24. N. El Mahallawy, A. Ahmed Diaa, M. Akdesir, H. Palkowski : Effect of Zn addition on the microstructure and mechanical properties of cast, rolled and extruded Mg-6Sn-xZn alloys. Materials Science and Engineering A, 680(October 2016), 47–53, 2017.
25. N. Hansen : Hall–Petch relation and boundary strengthening, Scripta Materialia, 51(8), 801-806, 2004.
26. Y. Ali, D. Qiu, B. Jiang, F. Pan, M. X. Zhang : Current research progress in grain refinement of cast magnesium alloys: A review article. Journal of Alloys and Compounds, 619, 639–651, 2015.
27. D. H. St. John, M. A. Qian, M. A. Easton, P. Cao, Z. Hildebrand : Grain refinement of magnesium alloys. Metallurgical and Materials Transactions A, 36(7), 1669-1679, 2005.
28. T. E. Quested, A. T. Dinsdale, A. L. Greer : Thermodynamic modelling of growth-restriction effects in aluminium alloys, Acta materialia, 53(5), 1323-1334, 2005.